

# Endocardial impedance mapping during circumferential pulmonary vein ablation of atrial fibrillation differentiates between atrial and venous tissue

Christopher C.E. Lang, MB, ChB, MD,<sup>a</sup> Filippo Gugliotta, BEng,<sup>a</sup> Vincenzo Santinelli, MD,<sup>a</sup> César Mesas, MD,<sup>a</sup> Takeshi Tomita, MD, PhD,<sup>a</sup> Gabriele Vicedomini, MD,<sup>a</sup> Giuseppe Augello, MD,<sup>a</sup> Simone Gulletta, MD,<sup>a</sup> Patrizio Mazzone, MD,<sup>a</sup> Francesco De Cobelli, MD,<sup>b</sup> Alessandro Del Maschio, MD,<sup>b</sup> Carlo Pappone, MD, PhD<sup>a</sup>

<sup>a</sup>From the Division of Arrhythmology and Cardiac Electrophysiology, San Raffaele Hospital, Milan, Italy, and

<sup>b</sup>Department of Diagnostic Radiology, San Raffaele Hospital, Milan, Italy.

**BACKGROUND** Circumferential pulmonary vein ablation (CPVA) is an effective treatment for atrial fibrillation (AF). Accurate left atrial (LA) mapping is essential for creating lesions at the LA–pulmonary vein (PV) junction, avoiding PV stenosis.

**OBJECTIVES** The purpose of this study was to establish whether endocardial impedance varies within the LA and PVs and whether it is a useful tool for mapping and ablation.

**METHODS** *Pilot Phase:* Three-dimensional LA maps were created using CARTO. Impedance (Z) was measured using a radiofrequency generator at multiple points in the LA, PV ostia (PVO), and deep PVs in 79 patients undergoing their first AF ablation (group 1) and 29 patients undergoing repeat CPVA (group 2). *Prospective Phase:* In an additional 20 patients, using pilot phase data, one operator defined catheter tip location as either LA or PVO based on CARTO and fluoroscopy. A second operator blinded to CARTO simultaneously did the same based on impedance at  $15 \pm 4$  points per patient.

**RESULTS** Group 1:  $Z_{LA}$  was  $99.4 \pm 9.0 \Omega$ .  $Z_{PVO}$  was higher ( $109.2 \pm 8.5 \Omega$ ), rising further as the catheter advanced into deep PV ( $137 \Omega \pm 18$ ).  $Z_{PVO}$  differed from  $Z_{LA}$  by  $9 \pm 4 \Omega$ . Group 2 had a lower  $Z_{LA}$  and  $Z_{PVO}$  compared with group 1 ( $P < .05$ ). Impedance monitoring differentiated between LA and PVO, with 91% specificity and sensitivity, 96% positive predictive value, and 81% negative predictive value. At 3-month follow-up, no patients had evidence of PV stenosis on magnetic resonance imaging.

**CONCLUSION** Impedance mapping reliably identifies the LA–PV transitional zone, facilitating AF ablation, and its use is associated with a low incidence of PV stenosis.

**KEYWORDS** Ablation, Atrial fibrillation; Impedance; Mapping

(Heart Rhythm 2006;3:171–178) © 2006 Heart Rhythm Society. All rights reserved.

## Introduction

Circumferential pulmonary vein ablation (CPVA) is an effective treatment for atrial fibrillation (AF).<sup>1,2</sup> The ability to understand and correctly reconstruct left atrial (LA) and

pulmonary vein (PV) anatomy is essential to deploy continuous effective ablation lines around the target regions at the pulmonary vein ostium (PVO)–LA junction. In our experience, one of the advantages of CPVA over other techniques is the absence of PV stenosis. However, other centers have reported a high incidence of PV stenosis after AF ablation using an electroanatomic approach.<sup>3</sup> To prevent this potentially serious complication, lesions must be deployed near the PVO–LA junction and not inside the vein.

We previously reported that the electrical impedance in the PVs is higher than in the LA,<sup>4,5</sup> and we have been using endocardial impedance to assist in both mapping and abla-

The first two authors contributed equally to the article and should be considered equal first author.

**Address reprint requests and correspondence:** Dr. Carlo Pappone, Division of Arrhythmology and Cardiac Electrophysiology, San Raffaele Hospital, 20132 Milan, Italy.

E-mail address: carlo.pappone@hsr.it.

(Received July 3, 2005; accepted October 12, 2005.)

**Table 1** Baseline patient characteristics

	Group 1 (n = 79)	Group 2 (n = 29)	P value
Age (yrs)	55.7 ± 9.3	59.1 ± 7.6	0.09
Sex (M/F)	47/31	15/14	0.42*
Weight (kg)	76.1 ± 8.1	78.7 ± 9	0.6
Left atrial volume (mL)	99.9 ± 37.4	89.5 ± 33.8	0.20

\*Chi-square test.

tion for several years. However, we have never formally described the use of this parameter, nor had we ever adopted a scientific approach to validating the use of impedance. Because the ability to distinguish between venous or atrial tissue may determine the risk of PV stenosis, we believed it was important to study the utility of this parameter, both to satisfy our own scientific curiosity and for the benefit of others wishing to use this technique.

The endocardial impedance ( $Z$ ) can be measured through the ablation catheter and is mainly a measure of the resistive components of the circuit composed of the ablation catheter and the tissues and organs through which the current must pass to the reference electrode. The impedance is affected by several factors: electrode contact with the endocardium,<sup>6,7</sup> position and size of the reference electrode,<sup>8</sup> and characteristics of the tissue in which it is in contact.<sup>9–13</sup>

The predetermined goals of this study were to formally describe the variation in impedance in the LA, PVO, and PVs in order to facilitate the accurate identification of PVO–LA junction and suitable sites for placement of safe and effective linear lesions; to determine whether impedance can reliably determine the catheter position relative to the PVO; and to establish whether impedance was affected by the ablation procedure.

## Patients and methods

### Pilot phase

Data were collected from 79 patients undergoing CPVA for the first time (group 1) and 29 patients with recurrent atrial fibrillation following previous CPVA who had elected to undergo repeat ablation (group 2). Baseline characteristics of patients are given in Table 1. Informed written consent was obtained from all patients, and the study was conducted in accordance with our institutional ethical guidelines. The ablation technique has been described in detail elsewhere.<sup>2,3</sup> Lesion strategy and pattern were standard for both groups. We performed CPVA, with a mitral valve to left inferior PV line and posterior lines connecting the left superior (LS) PV to right superior PV and/or left inferior PV to right inferior PV. Drag lesions were created using radiofrequency (RF) energy with a 100-W power limit and a temperature limit of 60°C. Procedures lasted 86 ± 17 minutes, including 20 ± 7 minutes for pre/post mapping and 51 ± 16 minutes for ablation.

### Impedance measurement circuit

A Stockert 100-W RF generator (Biosense Webster Inc, Diamond Bar, CA) was used to perform real-time impedance mapping (RTIM) with a Navi-Star 8Fr F-curve 8-mm-tip catheter (Biosense-Webster). The generator is equipped with an independent electrical circuit for continuous real-time impedance monitoring that produces a sinusoidal current of 2  $\mu$ A at a frequency of 50 kHz, which minimizes the complex polarization impedance at the electrode–tissue interface.<sup>6</sup> Catheter–tissue contact was assessed using several criteria: local activation time (patients in sinus rhythm), electrogram morphology, electrogram dV/dt, location stability, and, if necessary, fluoroscopy before acquisition of endocardial points. Location stability was confirmed by CARTO and stability of the impedance reading. Impedance values at stable positions were noted to vary by  $\pm 2 \Omega$ . The reference patch (Ref-Star, Biosense-Webster) was positioned on the patient's back between T2–T6 to minimize the impact of electrode position on impedance.

### Atrial and PV mapping and impedance measurement

Using the three-dimensional electroanatomic mapping system (CARTO, Biosense-Webster, Diamond Bar, CA, USA), the LA and PV anatomy was reconstructed, paying particular attention to the PVO regions. In each patient, impedance was monitored at a single point on the posterior wall of the LA for 30 seconds and was found to vary by  $\pm 2 \Omega$ . Deep in the PV, impedance varied with respiration by  $\pm 10 \Omega$  on average. Local impedance measurements ( $Z_{\text{RTIM}}$ ) were taken in the LA at a minimum of 10 points on the posterior wall, septum, roof, and mitral valve region. No significant differences were found between these regions, and the LA impedance ( $Z_{\text{LA}}$ ) was taken as the average of all points. The left atrial appendage (LAA) was distinguished by a higher-amplitude local electrogram ( $V_{\text{LAA}} > 1.5$  mV), organized activity in patients in AF, and the anterior position of the catheter as seen on CARTO in a left lateral view.

The atrial and PV anatomy was divided into three distinct zones based on anatomic location (defined by fluoroscopy and CARTO) and electrical characteristics: zone 1 (LA); zone 2—from the lip of the PVO (with detectable electrical signal  $0.05 \text{ mV} < V < 0.7 \pm 0.2 \text{ mV}$ ) until the point where the vein became electrically silent; and zone 3—deep PV where no electrical signal is detected ( $V$

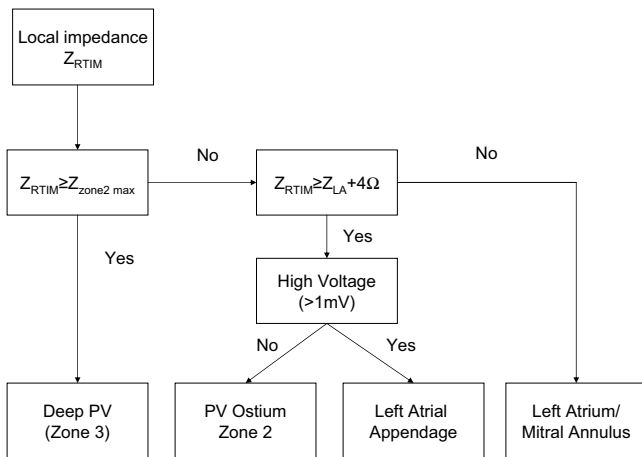


**Figure 1** Flowchart showing the decisional safety steps for determining the anatomic position in the left atrium (LA) according to RTIM.  $Z_{LA}$  = patient's mean left atrial (LA) impedance;  $Z_{RTIM}$  = impedance reading at each location.

<0.05V). The electrically silent portions of each vein were labeled using circular tubes on the CARTO system.

Impedance data were collected in all regions of the LA (zone 1) obtaining a mean impedance value ( $Z_{LA}$ ) (minimum of 10 points). The catheter was inserted deep into a PV (zone 3) where no signal was detected ( $V < 0.05$  mV) and impedance values collected in that area (average of 10 points,  $Z_{Z3}$ ). The catheter was withdrawn until a bipolar signal  $> 0.05$  mV was recorded. This point was determined as the start of zone 2, and, from this point, we collected the impedance values of zone 2 (average eight points per PVO,  $Z_{Z2}$ ) while withdrawing the catheter toward the LA. The catheter was noted to have entered the LA by a change in the plane of catheter movement or a sudden movement of the catheter tip as it fell out of the vein into the LA as seen on fluoroscopy and CARTO.

Postablation RTIM was repeated in both the LA and zone 2 of each PV as close as possible to sites of previous impedance measurement at a minimum distance of 5 mm from the RF lesion markers. Zone 3 measurements were not repeated because the impedance could vary widely with only small differences in depth and therefore were not considered reproducible. Impedance maps were created offline using manually entered values.

## Prospective phase

Using mean regional impedance values collected during the pilot phase, we created a flowchart to guide placement of lesions (Figure 1). To determine the sensitivity and specificity of an impedance cutoff of ( $Z_{LA} + 4 \Omega$ ), the impedance was recorded in an additional 20 patients at multiple points in the LA and PVO by an investigator blinded to the position of the ablation catheter. Based on impedance alone, one investigator would attempt to define whether the point was in the PVO (unsafe for RF application) or LA (safe for RF).

A second investigator determined whether a location was safe or unsafe for RF application, based on the catheter's anatomic position and local electrogram characteristics as seen on CARTO and/or fluoroscopy. A third operator who was responsible for the ablation procedure instructed the investigators when to take readings.

## Magnetic resonance imaging

At  $3 \pm 1$  months after ablation, all 20 patients from the prospective phase underwent contrast-enhanced magnetic resonance angiography of the PVs using a 1.5-T superconducting magnet (Gyrosan Intera, release 9, Philips Medical Systems, Eindhoven, Netherlands).

## Statistical analysis

Statistic analysis was performed using SPSS10 (Chicago, Illinois) for Windows. Paired and unpaired t-tests were used to test the significance of differences in preablation and postablation impedance and between groups, respectively. The receiver operator characteristic (ROC) was determined comparing the local impedance at individual points ( $Z_{RTIM}$ ) minus ( $Z_{LA} + 4 \Omega$ ) compared against the suitability (safe = 1, unsafe = 0) of each site for RF application as determined by electroanatomic mapping. Data are presented as mean  $\pm$  SD.

## Results

### Patient characteristics

Baseline patient characteristics are given in Table 1. There was no correlation between patient characteristics and endocardial impedance. In particular, there was no relationship between patient weight and mean endocardial impedance. However, because data on patient height were not available, we cannot exclude a weak relationship between endocardial impedance and body mass index.

### Preablation impedance

Impedance data for each of the zones were normally distributed. In both groups, significant differences were detectable between the three predefined zones ( $P < .0001$  for zone 2 of each PV vs LA in both groups). Paired t-tests were used to compare the impedance in individual veins, but there was no significant difference between any of the veins. When all patients were grouped together the absolute values for each zone 2 were as follows: right upper PV  $106.8 \pm 10.5 \Omega$ ; right lower LPV  $107.7 \pm 12.8 \Omega$ ; left upper PV  $106.0 \pm 9.7 \Omega$ ; left lower PV  $106.6 \pm 10.3 \Omega$ . Mean LA impedance ( $Z_{LA}$ ) was  $99.4 \pm 9.0 \Omega$  and  $95.9 \pm 7 \Omega$  ( $P < .05$ ) in groups 1 and 2, respectively. Upon entering zone 2, impedance rose

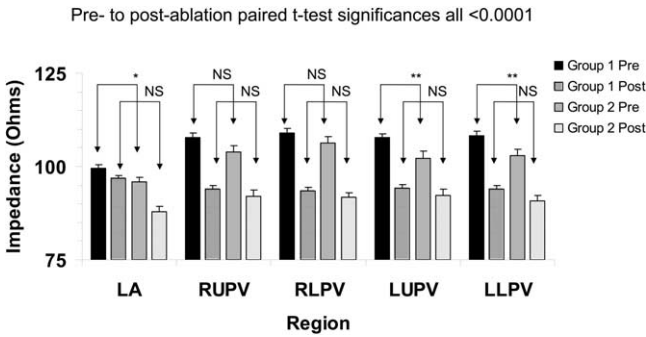


**Figure 2** Preablation and postablation variation in impedance. Chart shows the relative differences in impedance in the left atrium (LA) and each pulmonary vein (PV) ostium and their statistical significance between the two study groups before and after ablation. Significance was calculated using paired and unpaired t-tests for intragroup and intergroup differences, respectively. LLPV = left lower pulmonary vein; LUPV = left upper pulmonary vein; RLPV = right lower pulmonary vein; RUPV = right upper pulmonary vein. \* $P < .05$ ; \*\* $P < .001$ .

to  $109.2 \pm 8.5 \Omega$  and  $101.3 \pm 9 \Omega$  respectively ( $P < .005$ ). Impedance continued to rise rapidly upon catheter advancement in zone 3, with mean impedances in these regions of  $137 \pm 18 \Omega$  and  $128 \pm 17 \Omega$ , respectively ( $P = .09$ ). A small change in the depth of the catheter in zone 3 could result in a large difference in impedance. The gradient between LA and zone 2 was more marked in the CPVA-naive group in the left but not in the right PVOs. The mean impedance gradients between LA and zone 2 were  $9.0 \pm 4.1 \Omega$  and  $7.1 \pm 3.9 \Omega$  ( $P = NS$ ) for groups 1 and 2, respectively. These data are summarized in Figure 2 and illustrated in Figure 3. The impedance in the LAA ( $Z_{LAA}$ ) was higher

than the rest of the LA in groups 1 and 2 by  $4.4 \pm 3.3 \Omega$  and  $3.3 \pm 3.2 \Omega$  in both groups ( $P < .01$ ).

**Postablation impedance**

Following CPVA, impedance reduced significantly in all regions in both groups, and the difference between preablation and postablation impedance values was highly statistically significant in all regions in both groups ( $P < .0001$ ). The average absolute drop in LA impedance was  $9.8 \pm 4 \Omega$  and  $8 \pm 5 \Omega$  in groups 1 and 2, respectively, and between 9 and 15  $\Omega$  and between 9 and 12  $\Omega$  in zone 2 in groups 1 and 2, respectively, depending on the PV. The relative reduction in impedance was greatest in zone 2, thus reducing the gradient between LA and PVO. This phenomenon is illustrated in Figure 4.

**Impedance guided ablation and PV stenosis**

Using the impedance data from these populations, a decision algorithm was developed to help determine catheter position relative to the PV-LA junction (Figure 1). As the mean difference in impedance between the LA and zone 2 was 9  $\Omega$ , we assumed that a rise in impedance  $>4 \Omega$  above  $Z_{LA}$  represented the midpoint of the PV-LA transitional zone. As long as the impedance was  $\leq [Z_{LA} + 4 \Omega]$ , we could expect to be on the atrial aspect of the transitional zone, and this value was used as an upper limit for lesion deployment. Using this algorithm, an additional 20 patients underwent mapping prior to CPVA. After standard impedance mapping to calculate  $Z_{LA}$ , a mean of  $15 \pm 4$  location points was collected per patient. For each point, one inves-

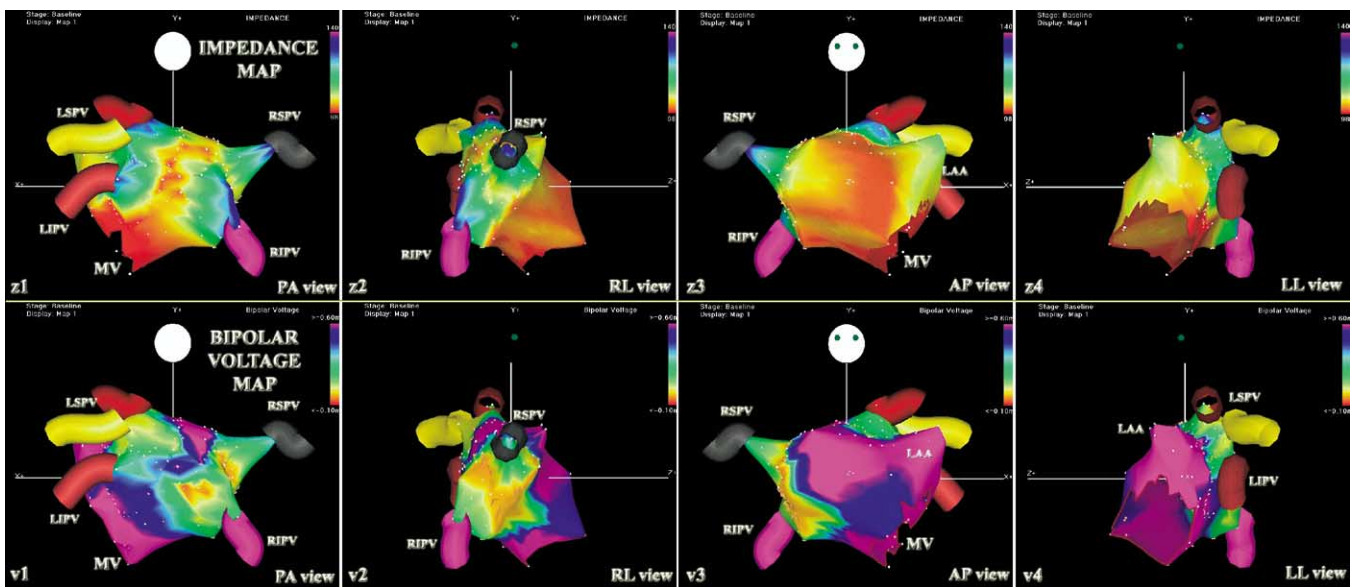


**Figure 3** Preablation impedance maps (upper panels, z1–z4) and bipolar voltage map (lower panels, v1–v4) in different views. In this case BVM with a manual color range from 0.10 mV (red) to 0.6 mV (violet), and ZM with an automatic color range from 98 $\Omega$  (red) to 140 $\Omega$  (violet) both help in identifying PVO-LA junction. The PV ostial regions appear green both in ZM and BVM. Lower voltages are recorded both in Zone 3 and in Zone 2. Higher impedances and lower voltages are recorded in Zone 2 and 3.

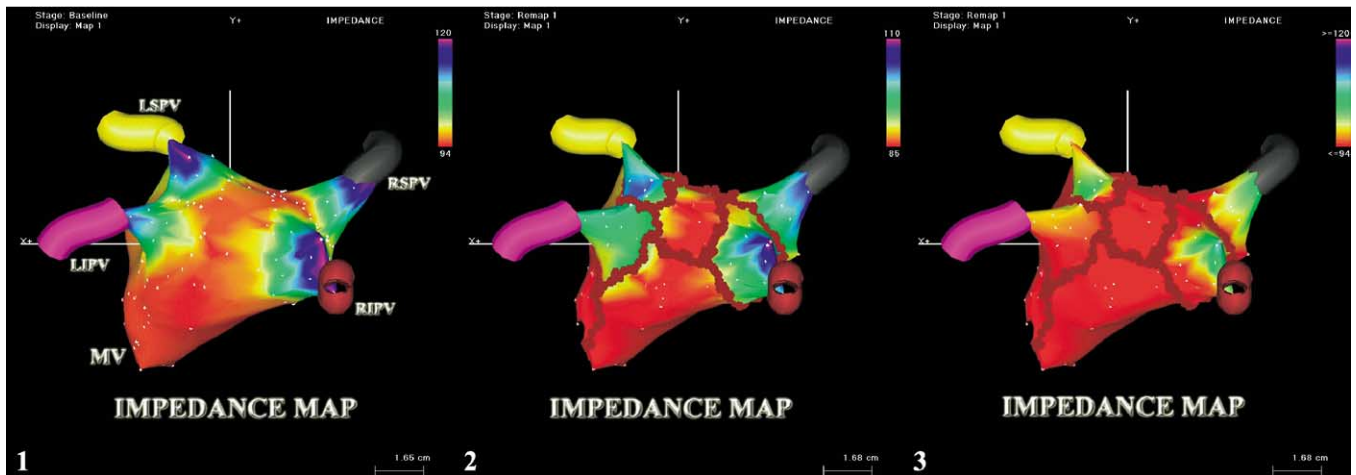


**Figure 4** **Panel 1:** Preablation impedance map (ZM) using an automatic color range from 94 to 120  $\Omega$ . **Panel 2:** Postablation ZM with automatic color range from 85 to 110  $\Omega$  demonstrating that the left atrium (LA)–pulmonary vein ostium (PVO) impedance gradient still exists following ablation. **Panel 3:** Same postablation ZM as panel 2 but using a manual scale matching that of panel 1 demonstrating the absolute reduction in impedance and the LA–PVO gradient.

tigator blinded to catheter position on CARTO and fluoroscopy estimated whether the ablation catheter was in the LA (safe for ablation) or in the PVO/deep PV (unsafe) at each point using an impedance limit of (mean LA impedance + 4  $\Omega$ ). A second investigator who was blinded to impedance readings determined whether the catheter was in the LA, PVO, or PV at these same points based on the local electrograms and catheter position relative to the PVO as seen on fluoroscopy and CARTO geometry. Of 324 points sampled, impedance alone correctly identified 212 (91%) of 232 points determined as safe based on CARTO data and 84 (91%) of 92 regarded as unsafe (PVO). Positive and negative predictive values were 96% and 81%, respectively. If the catheter was being dragged during RF application and a rise  $\geq 4$   $\Omega$  relative to the previous locus was observed, this was an indication to stop RF, check catheter position, and move to an adjacent area of lower impedance. It was possible to successfully perform the ablation using the impedance cutoff criteria in all patients without any significant adjustment of the lesion sets (i.e., no visible deviations from normal on the postablation maps). No patient had evidence of PV stenosis on contrast-enhanced magnetic resonance angiography at 3 months. Using the difference between local and mean LA impedance and the position data from CARTO, the ROC was constructed. The area under the curve was 0.916 (95% confidence limits 0.875–0.958,  $P < .001$ ).

## Discussion

Impedance monitoring is used often in the electrophysiology laboratory. Sudden rises in impedance during RF application often indicate carbonization on the catheter tip, and a drop in local impedance usually is seen after successful lesion creation. During mapping, higher endocardial

impedance is seen when the catheter is in contact with or inserted into venous structures such as the coronary sinus or other cardiac veins. The LA–PV anatomy is complex,<sup>14</sup> posing problems for operators attempting to isolate the PVs, whether a segmental or an anatomic approach is used. At our center, we have routinely used impedance as a guide for catheter positioning for several years, and we believe that this is one potential explanation for the absence of clinical PV stenosis in our large series of patients.

## Impedance variation and tissue type

We have shown that, during baseline mapping, impedance rises significantly as the ablation catheter enters the PVO (zone 2) and that, when located deep inside the electrically silent portion of the vein, impedance is much higher. Several studies have shown that there is a gradual transition in histology from the muscular atrium to the venous tissue.<sup>15–17</sup> The PVO tissue is complex, having myocardial fibers traveling in multiple directions. Previous studies have shown that both fiber direction<sup>18</sup> and fibrosis<sup>19</sup> are associated with higher tissue resistivities. The observed difference in impedance between LA and PVO may reflect these transitional tissue characteristics. Other investigators have described fractionated electrograms around the PVO<sup>20,21</sup> and have targeted these electrograms for ablation with considerable success in the treatment of AF. We do not specifically target these fractionated areas, but they can be a useful guide to the proximity to the PV–LA junction and are frequently present at sites designated for RF application.

Case reports of PV stenosis or occlusion occurring with the circumferential approach to AF ablation are rare. However, the Johns Hopkins group describes a case of hemoptysis following circumferential AF ablation that was shown to be due to the occlusion of a small sub-branch of a right inferior PV.<sup>22</sup> It is possible that when high impedance

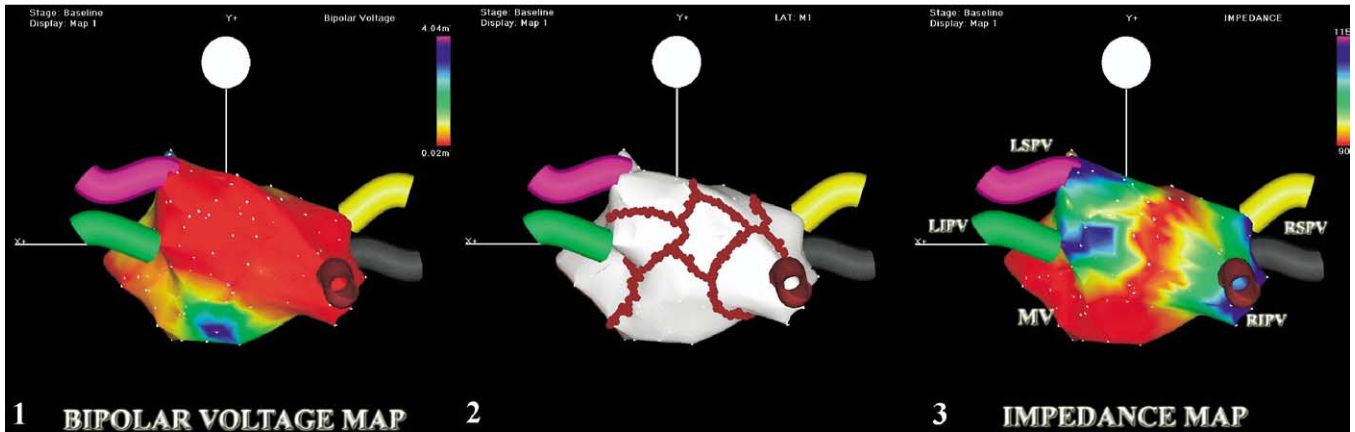


**Figure 5** Bipolar voltage (left), lesion location (middle), and impedance maps (right) from a patient with extensive low-voltage areas (red). Although the voltage map is not helpful for identifying pulmonary vein ostia, impedance measurements helped to differentiate between left atrium and pulmonary vein ostia. LIPV = left inferior pulmonary vein; LSPV = left superior pulmonary vein; MV = mitral valve; RIPV = right inferior pulmonary vein; RSPV = right superior pulmonary vein.

values are detected, the catheter tip is in contact with the ostium of a small branch; therefore, we recommend that ablation not be performed at points where impedance is higher than expected or permitted by the algorithm. However, in our experience, routine use of impedance does not prohibit the completion of a successful lesion set; it merely forces a slight “detour” around the area of higher impedance.

**Impedance mapping vs voltage mapping in the LA**

Using impedance values collected from catheter locations ( $Z_{RTIM}$ ), we created offline impedance maps of the LA. Close monitoring of impedance readings can guide mapping and ablation, and a combination of voltage and impedance data can be used to select suitable sites for ablation, although we rely more on impedance, particularly in patients with extensive low-voltage regions in the LA and PVO (Figure 5), or disorganized electrical activity as seen in patients in AF.

**Acute and chronic reduction in atrial impedance**

Endocardial impedance falls during CPVA at sites remote from lesions. This most likely is due to the creation of interstitial edema in response to injury. Other studies have shown that osmotically induced increases in the extracellular volume, modeling tissue edema, cause a decrease in myocardial tissue impedance.<sup>23</sup> Magnetic resonance imaging performed a few days after CPVA shows extensive edema throughout the posterior wall, PVO, and interatrial septum (Figure 6). Our data also support a possible chronic reduction in impedance following CPVA, as group 2 patients had lower LA and overall zone 2 impedance preablation and a lower LA–PVO impedance gradient. It could be that the observed difference was related to measurement at sites of previous ablation, although this is unlikely as zone 2 points were taken inside the ostia, some distance from the

perimetric external circumferential lines. Previous studies on animal models of myocardial infarction have shown that infarcted tissue has lower impedance.<sup>12,13</sup> This may be due to a relatively greater proportion of extracellular matrix and fewer myocytes. Others have shown that fibrosis affects tissue impedance because of loss of cell-to-cell communication.<sup>19</sup> Repeat evaluation of patients in this study would be required to determine whether the observed acute reduction in impedance is maintained in the long term.

**Impedance and PV stenosis**

This article represents the formal description of LA endocardial impedance mapping for assisting AF ablation. In this

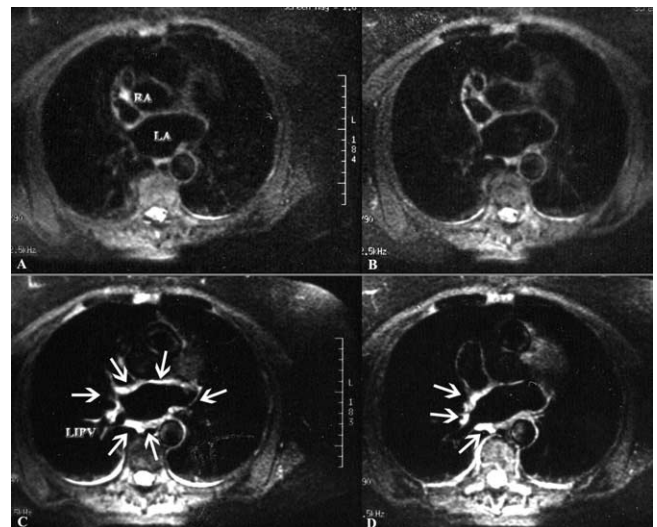


**Figure 6** Magnetic resonance imaging at the level of the left atrium (LA) before (A, B) and 1 day after (C, D) radiofrequency ablation. Postablation, extensive high signal intensity and wall thickening are evident in the atrial wall and at the junction with the left inferior pulmonary vein (LIPV) due to the presence of edema (arrows). RA = right atrium.

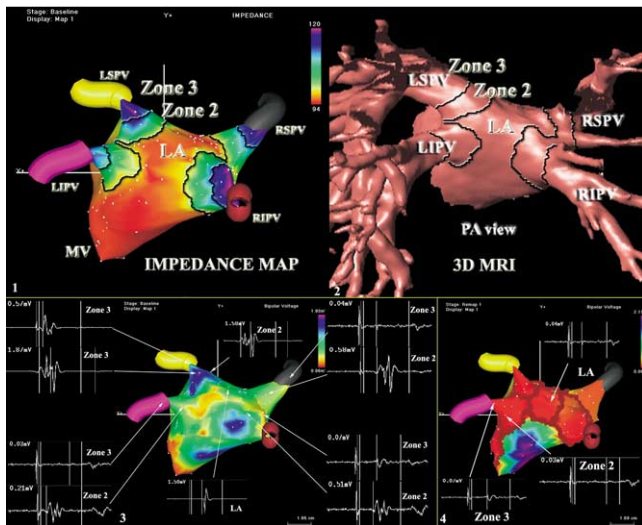


**Figure 7** **Panel 1:** CARTO offline impedance map. **Panel 2:** Three-dimensional reconstruction from magnetic resonance imaging (3D MRI) of the same patient in the posteroanterior (PA) view. The three zones based on impedance are highlighted with *dark lines*. The similarity between the 3D CARTO map and the 3D MRI reconstruction is notable. **Panels 3, 4:** Electrogram *insets* illustrate the variation in amplitude and morphology in local electrograms in the atrial, ostial, and deep venous region that can be found in different veins. In contrast, there is little variation in impedance between the corresponding areas in different veins (panel 1). LA = left atrium; MV = mitral valve; LIPV = left inferior pulmonary vein; LSPV = left superior pulmonary vein; RIPV = right inferior pulmonary vein; RSPV = right superior pulmonary vein.

study, we were able to detect suitable sites for ablation with high sensitivity, specificity, and positive predictive value using impedance alone. When used in combination with a three-dimensional map, impedance can become a valuable surrogate marker for the presence of transitional or venous tissue at the catheter location. It may be that sites that appeared to be safe according to anatomy but had a higher than expected impedance may represent regions where small venous branches are arising<sup>14,22</sup> (Figure 7) and therefore were misclassified as safe by CARTO. Our findings are in keeping with a previous article study on impedance in the LA and PVs.<sup>24</sup> These investigators assessed the specificity of a sudden rise in impedance  $>4 \Omega$  for detecting when the catheter fell into the PV during RF application and found a high sensitivity and positive predictive value. In this study, we assessed the usefulness of impedance in mapping and identifying atrial and venous tissue. From the data, we have been able to construct a robust algorithm to assist mapping and ablation. Using invasive techniques such as intracardiac echocardiography, it is possible to reduce the incidence of PV stenosis,<sup>5</sup> although impedance data are readily available and can be used to guide ablation. The small number of patients in the prospective phase of the study in whom PV stenosis was excluded following ablation precludes any significant conclusion regarding the actual incidence of PV stenosis. However, we have been using impedance to guide ablation for several years and have not knowingly had a

single case of PV stenosis after several thousand cases. The CPVA approach has not been modified in this study because of the use of impedance. The data presented merely represent the formal description of the use of impedance, and the prospective phase represents validation of  $\geq 4 \Omega$  cutoff. Hopefully, other centers can utilize this information, including impedance monitoring and mapping in AF ablation procedures.

## Conclusion

This study formally describes the impedance characteristics of the LA–PV complex in patients undergoing AF ablation. Impedance monitoring can be used to reliably distinguish between LA and PVO, increasing our ability to safely ablate within the LA. Impedance may prove to be more reliable than three-dimensional mapping alone for detecting the presence of minor veins, which also are at high risk for stenosis should RF energy be inadvertently delivered at their ostium.<sup>22,25</sup> Use of impedance mapping may help reduce the incidence of PV stenosis following CPVA. RF energy should be delivered in the periostial region only when the impedance value is comparable to that of the LA ( $\leq 4 \Omega$  above LA mean) to avoid ablation within the PV and the associated risk of PV stenosis. The ability to create online impedance maps would enhance our ability to identify the LA–PV junction and perform LA ablations.

## References

- Pappone C, Santinelli V, Manguso F, Vicedomini G, Gugliotta F, Augello G, Mazzone P, Tortoriello V, Landoni G, Zangrillo A, Lang C, Tomita T, Mesas C, Mastella E, Alfieri O. Pulmonary vein denervation enhances long-term benefit after circumferential ablation for paroxysmal atrial fibrillation. *Circulation* 2004;109:327–334.
- Pappone C, Rosanio S, Augello G, Gallus G, Vicedomini G, Mazzone P, Gulletta S, Gugliotta F, Pappone A, Santinelli V, Tortoriello V, Sala S, Zangrillo A, Crescenzi G, Benussi S, Alfieri O. Mortality, morbidity and quality of life after circumferential pulmonary vein ablation for atrial fibrillation. *J Am Coll Cardiol* 2003;42:185–197.
- Saad E, Rossillo A, Saad C, Martin DO, Bhargava M, Erciyes D, Bash D, Williams-Andrews M, Beheiry S, Marrouche NF, Adams J, Pisano E, Fanelli R, Potenza D, Raviello A, Bonso A, Themistoclakis S, Brachmann J, Saliba WI, Schweikert RA, Natale A. Pulmonary vein stenosis after radiofrequency ablation of atrial fibrillation. functional characterization, evolution, and influence of the ablation strategy. *Circulation* 2003;108:3102–3107.
- Pappone C, Rosanio S, Oretto G, Tocchi M, Gugliotta F, Vicedomini G, Salvati A, Dicandia C, Mazzone P, Santinelli V, Gulletta S, Chierchia S. Circumferential radiofrequency ablation of pulmonary vein ostia. A new anatomic approach for curing atrial fibrillation. *Circulation* 2000;102:2619–2628.
- Pappone C, Oretto G, Rosanio S, Vicedomini G, Tocchi M, Gugliotta F, Salvati A, Dicandia C, Calabro MP, Mazzone P, Ficarra E, Di Gioia C, Gulletta S, Nardi S, Santinelli V, Benussi S, Alfieri O. Atrial Electro-anatomic recording after circumferential radiofrequency pulmonary vein ablation. Efficacy of an anatomic approach in a large cohort of patients with atrial fibrillation. *Circulation* 2001;104:2539–2544.

6. Cao H, Speidel M, Tsai J, Lysel M, Vorperian V, Webster J. FEM Analysis of predicting electrode myocardium contact from RF cardiac catheter ablation system impedance. *IEEE Trans Biomed Eng* 2002; 49:520–526.
7. Cao H, Tungjitkusolmun S, Choy Y, Tsai J, Vorperian V, Webster J. Using electrical impedance to predict catheter-endocardial contact during RF cardiac ablation. *IEEE Trans Biomed Eng* 2002;49:247–253.
8. Nath S, Di Marco J, Gallop R, McRury I, Haines D. Effects of dispersive electrode position and surface area on electrical parameters and temperature during radiofrequency catheter ablation. *Am J Cardiol* 1996;77:765–767.
9. Schwan H, Kay C. Specific resistance of body tissue. *Circ Res* 1956; 4:664–670.
10. Abildskov J, McFee R. Resistivity of body tissues at low frequencies. *Circ Res* 1963;12:40–50.
11. Cinca J, Warren M, Carreno A, Tresanchez M, Armadans L, Gomez P, Soler-Soler J. Changes in myocardial electrical impedance induced by coronary artery occlusion in pigs with and without preconditioning. *Circulation* 1997;96:3079–3086.
12. Warren M, Bragos R, Casas O, Rodriguez-Sinovas A, Rosell J, Anivarro I, Cinca J. Percutaneous electrocatheter technique for on-line detection of healed transmural myocardial infarction. *Pacing Clin Electrophysiol* 2000;23:1283–1287.
13. Wolf T, Gepstein L, Hayam G, Zaretzky A, Shofty R, Kirshenbaum D, Uretzky G, Oron U, Ben-Haim SA. Three-dimensional endocardial impedance mapping: a new approach for myocardial infarction assessment. *Am J Physiol Heart Circ Physiol* 2001;280:H179–H188.
14. Mansour M, Holmvang G, Sosnovik D, Migrino R, Abbara S, Ruskin J, Keane D. Assessment of pulmonary vein anatomic variability by magnetic resonance imaging: implications for catheter ablation techniques for atrial fibrillation. *J Cardiovasc Electrophysiol* 2004;15:387–393.
15. Nathan H, Eliakim M. The Junction between the left atrium and the pulmonary veins: an anatomic study of human hearts. *Circulation* 1966; 34:412–422.
16. Saito T, Waki K, Becker A. Left myocardial extension onto pulmonary veins in humans. Anatomic observations relevant for atrial arrhythmias. *J Cardiovasc Electrophysiol* 2000;11:888–894.
17. Moubarak JB, Rozwadowski JV, Strzalka CT, Buck WR, Tan WS, Kish GF, Kisiel T, Fronc HC, Maloney JD. Pulmonary veins-left atrial junction: anatomic and histologic study. *Pacing Clin Electrophysiol* 2000;23(11 Pt 2):1836–1838
18. Kucera J, Rudy Y. Mechanistic insights into very slow conduction in branching cardiac tissue. *Circ Res* 2001;89:799–807.
19. Spach M, Boineau J. Microfibrosis produces electrical load variations due to loss of side to side cell connections: a major mechanism of structural heart disease arrhythmias. *Pacing Clin Electrophysiol* 1997; 20:397–413.
20. Nademanee K, McKenzie J, Kosar E, Schwab M, Sunsaneewitayakul B, Vasavakul T, Khunnawat C, Ngarmukos T. A new approach for catheter ablation of atrial fibrillation: mapping of the electrophysiologic substrate. *J Am Coll Cardiol* 2004;43:2044–2053.
21. Pachon JC, Pachon EI, Pachon JC, Lobo T, Pachon MZ, Vargas NA, Pachon DQ, Lopez FJ, Jatene AD. A new treatment for atrial fibrillation based on spectral analysis to guide the catheter RF-ablation. *Europace* 2004;6:590–601.
22. Vasamreddy CR, Jayam V, Bluemke D, Calkins H. Pulmonary vein occlusion: an unanticipated complication of catheter ablation of atrial fibrillation using the anatomic circumferential approach. *Heart Rhythm* 2004;1:78–81.
23. Fleischhauer J, Lehman L, Kleber A. Electrical resistances of interstitial and microvascular space as determinants of the extracellular electrical field and velocity of propagation in ventricular myocardium. *Circulation* 1995;92:587–594.
24. Cheung P, Hall B, Chugh A, Good E, Lemola K, Han J, Tamirisa K, Pelosi F Jr, Morady F, Oral H. Detection of inadvertent catheter movement into a pulmonary vein during radiofrequency catheter ablation by real-time impedance monitoring. *J Cardiovasc Electrophysiol* 2004;15:674–678.
25. Leite L, Asirvatham S, Monahan KH, Shen WK, Rea RF, Hammill SC. Progression of pulmonary vein stenosis in patients following focal atrial fibrillation ablation (abstr). *Pacing Clin Electrophysiol* 2002;25:559.